Available online at www.sciencedirect.com
ScienceDirect
Ceramics International 35 (2009) 3495–3502
CERAMICS INTERNATIONAL
www.elsevier.com/locate/ceramint

Short communication

Wear properties and microstructures of alumina matrix composite ceramics used for drawing dies

Yang Xue-feng*, Ze Xiang-bo, Wang Hong-yan, Wang Hui

School of Mechanical Engineering, University of Jinan, Jinan 250022, China

Received 3 November 2008; received in revised form 10 February 2009; accepted 19 April 2009
Available online 21 May 2009

Abstract

The alumina matrix ceramics used for drawing dies were prepared by hot-press sintering method. The ceramics materials were made of Al_2O_3/TiC, Al_2O_3/(W,Ti)C and Al_2O_3/Ti(C,N). Mechanical and friction properties of these materials were tested and measured. The experiments for testing friction properties were carried on wear and tear machine. Mechanisms of frictions were analyzed with scanning electron microscope. Results showed that the alumina matrix composite ceramics have good physical and mechanical properties for used as drawing dies. Measured friction coefficients of alumina matrix composite ceramics showed a trend of decline and kept the value of 0.4–0.5 with the rotating speed of 550 rpm. Alumina matrix composite ceramics have smaller wear rate, while the wear rates of Al_2O_3/TiC and Al_2O_3/(W,Ti)C decrease gradually with a rising rotation speed. The wear of alumina matrix ceramics was severe at deformation zone. The primary wear behaviors of alumina matrix ceramics are scraping and furrowing. Even though the mechanisms for wear different, abrasive and adhesive wear were found to be the predominant wear mechanisms for the ceramic drawing die.

Keywords: B. Surfaces; C. Wear resistance; D. Al_2O_3; E. Wear parts

1. Introduction

In wire drawing industry, the wire drawing die is the important wasting mould used for wire, cable, welding rod, etc. The expense of dies is about 50% of the all drawing process. The deformation zone and invariable zone of die touch drawn wire in drawing process. The sliding friction happened between die and wire in inner hole. The deformation zone and invariable zone are under high temperature and high pressure [1,2]. The acute wear and friction inside inner hole could shorten the longevity of dies, reduce the dimension precision of wire and increase the surface roughness [3–5].

The alumina matrix ceramic materials have excellent general mechanics properties in wear resistance, oxidation resistance and corrosion resistance, thus making them an ideal material for excellent materials used for wire drawing dies [6–7].

2. Experimental

2.1. Preparation of the materials and its mechanical properties

The alumina matrix ceramic composites were made of Al_2O_3/TiC, Al_2O_3/(W,Ti)C and Al_2O_3/Ti(C,N). The α-Al_2O_3 powder, with a purity of more than 99.9% and density of 3.99 g/cm^3 has an averaged diameter of less than 0.5 μm. The purity of TiC powder was more than 99.8%, its density was 4.25 g/cm^3, its average diameter was shorter than 0.5 μm. The purity of (W,Ti)C and Ti(C,N) powder was both more than 99.8%, their densities were 9.49 g/cm^3 and 5.15 g/cm^3 respectively, their average diameters were smaller than 0.8 μm. The mechanical properties of these materials have been listed in Table 1. The Al_2O_3/TiC, Al_2O_3/(W,Ti)C and Al_2O_3/Ti(C,N) raw materials have been mixed in ball milling canister with ethanol and ceramic small ball for 48 h, the phase contents of Al_2O_3/(W,Ti)C ceramic composites were 45 vol.% Al_2O_3 and 55 vol.% TiC, the phase contents of Al_2O_3/TiC ceramic composites were 66 vol.% Al_2O_3 and 34 vol.% (W,Ti)C, the phase contents of Al_2O_3/Ti(C,N) ceramic composites were

* Corresponding author. Tel.: +86 13075362913.
E-mail address: me_yangxf@ujn.edu.cn (X.-f. Yang).

0272-8842/$36.00.
doi:10.1016/j.ceramint.2009.04.012

Table 1
The mechanical properties of raw materials.

Materials	Density (g/cm^3)	Hardness (GPa)	Elastic modulus (GPa)	Thermal expansivity ($\times 10^{-6}\ K^{-1}$)	Poisson's ratio	Granularity (μm)	Material conductivity (W/(m K))
Al_2O_3	3.99	21	400	8.4	0.26	0.5	30.2
TiC	4.93	30	460	7.74	0.19	0.5	24.28
(W,Ti)C	9.49	30	570	5.58	0.2	0.8	27.12
Ti(C,N)	5.15	26-32	521	8.61	0.21	0.8	21.26

50 vol.% Al_2O_3 and 50 vol.% Ti(C,N). After roasting in dryness box, the mixed materials must be sifted in screen at flowing N_2 atmosphere and then have been reserved under N_2 atmosphere for further use.

The ceramic composites used for drawing dies were prepared by hot pressing sintering method. The sintering temperature was 1700–1800 °C, the pressure was 40 MPa, materials were kept under this condition for 10–30 min, and the sintering atmosphere was N_2. After that process, the prepared composite ceramics were sliced into 3 mm × 4 mm × 36 mm specimens, their densities were measured by drainage method; their hardness were surveyed used Veckers HV120 sclerometer, loading force was 10 N, the retaining time was 10 s; their flexure strengths were surveyed by three-point winding method, the span distance was 20 mm, the loading rate was 0.2 mm/min; their fracture toughness were measured by impress means, the force of impress was 196 N, the retaining time was 15 s, the length of impress was measured by 400 times microscope. The microstructures of composites were observed by HITACHI S-570 scanning electron microscope.

2.2. The experiment of friction properties

The experiment was carried with a MRH-3 high speed wear test machine made by Jinan test machine factory. The machine was sliding friction type between ring and lump for testing the ceramic composites friction coefficient and wear rate in the condition of given load and rotation speed. The lumps were prepared by Al_2O_3/TiC, Al_2O_3/(W,Ti)C and Al_2O_3/Ti(C,N) ceramic composites, their three dimensions were 15 mm (length) × 12 mm (width) × 5 mm (height), which have been processed with rigorous grinding and burnishing. The ring was made of 45# steel which hardness was HRC 45 ± 3, its outer diameter was 50 mm, inner diameter was 35 mm, and width was 13 mm. The work condition was dry friction with no lubrication. The lump was fixed by a fixture instrument, the ring rotated at the speed of 100–550 rpm, the load direction was along the normal-line of the friction surface. The sketch of equipment was shown in Fig. 1.

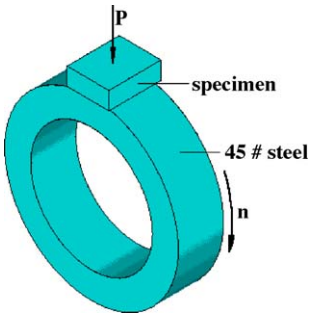

Fig. 1. The sketch of wear and tear experiment.

The wear and tear of Al_2O_3 matrix ceramic composites were weighed by the high precision electronic scales, the decrease of weight indicated the volume of wear, and then the wear rate was figured out. The precision of the electronic scales was 0.00001 g. The testing period was 30 min every time. The wear rate was calculated by formula (1):

$$W = \frac{\Delta\omega}{2\pi R t n \mu P \rho} \tag{1}$$

Δw is wear and tear volume (g); ρ is the density of the sample(g/cm^3); R is average friction radius, that is the distance between the center of the lump and the rotating axle of the ring (m); t is the duration of time (min); n is the rotation speed of the ring (rpm); μ is average friction coefficient; P is the force on the lump (N).

2.3. Fabrication of ceramics mould and setup for its property testing

A set of graphite mould suitable for the preparation of the ceramic drawing die was designed. The shape of inner hole of die was made in sintering and this method was convenient to form inner hole structures. The key technologies for the burnishing ceramic die were studied, the polishing particles was 0.5 μm B_4C, the polishing tool was cast iron, the lubrication medium was mineral oil and the polishing method was manually combined with some automatic way. The interference between steel holder and ceramic die core was obtained by theoretic calculation, and its value was 15.7–72.4 μm. The dimension and the tolerance of steel holder were deduced and the structure of steel holder was designed. The assemblage temperature was calculated by analyzing the interference and surface roughness. Results showed that the suitable assemblage temperature was 250 °C. The steel holder and ceramics dies

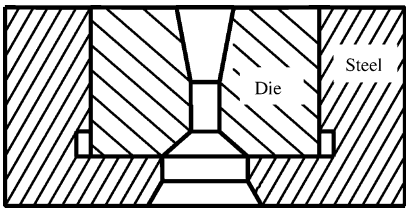

Fig. 2. The design structure of the ceramic dies.

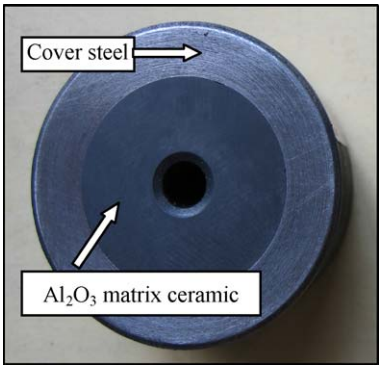

Fig. 3. The wire drawing die.

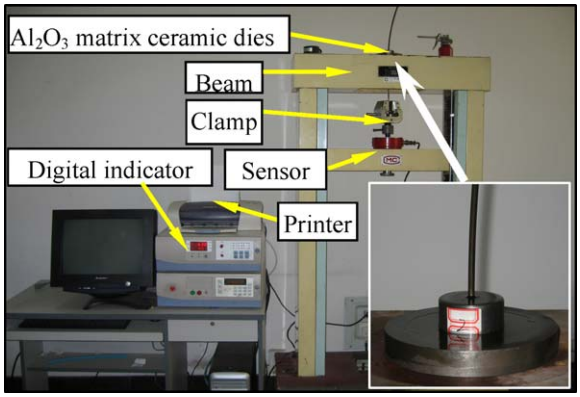

Fig. 4. The wire drawing test equipment.

core could be well assembled under these conditions. The ceramic die was successfully developed. The main properties of the ceramic dies were evaluated. The design structures of ceramic dies were as Fig. 2. The prepared Al_2O_3 matrix ceramic dies were showed as Fig. 3.

According to the working process of drawing machine, the test equipment platform was designed for testing drawing properties of Al_2O_3 matrix ceramic dies. The drawn wire was 65Mn steel; its diameter was 4.5 mm and then changed to 4 mm after drawing process, with the reduction ratio of 21%. The test equipment suitable for wire drawing was shown in Fig. 4. Wire drawing dies appear sliding friction with wire in drawing process. The friction and wear behaviors of die interconnect with inner hole closely. After experiment of drawing, the dies were cut open by thread cutter through symmetry axis. It was washed in ultrasonic launder by grain alcohol and then dried and preserved in airproof environment. The microstructure of dies samples was investigated by SEM micrographs.

3. Results and discussion

3.1. The mechanical properties of alumina matrix composites

The mechanical properties of composites dies were listed in Table 2. It showed that the Al_2O_3/TiC, Al_2O_3/(W,Ti)C and Al_2O_3/Ti(C,N) had good hardness and flexure strength. All mechanical properties of Al_2O_3 matrix ceramic dies were suitable for making drawing dies.

The microstructures of polishing surfaces of Al_2O_3 matrix ceramic dies were shown in Fig. 5. Fig. 5(a) was the polishing surface of Al_2O_3/TiC, Fig. 5(b) was the polishing surface of Al_2O_3/(W,Ti)C, Fig. 5(c) was the polishing surface of Al_2O_3/Ti(C,N). Results showed that the Al_2O_3 matrix formed spatial reticulation structure with addition phase and the tough surfaces contacted each others tightly between Al_2O_3 matrix and addition phase. The polished surfaces had compact structures and no micro-cracks.

The Al_2O_3 matrix composites brought on transgranular fracture in crack process because of spatial reticulation structure. The micrographs of fracture surfaces of Al_2O_3 matrix were shown in Fig. 6. It indicated that the grain of Al_2O_3 matrix composites were uniform and formed ripple and strip-sowing structure obviously after some micro crystal peel off. The microstructures of Al_2O_3 matrix composites belonged to coexistence of brittle fracture and transgranular fracture.

3.2. The friction properties of alumina matrix ceramic dies

The friction coefficient curves of Al_2O_3/TiC, Al_2O_3/(W,Ti)C and Al_2O_3/Ti(C,N) were shown in Fig. 7 which was tested with an increasing ring rotating speed and the load was fixed as 90 N. From this figure, it could be seen that the friction coefficients of three materials varied a lot however with a dropping trend. At low velocity, the friction coefficient of Al_2O_3 matrix composites had a higher of 0.7. And then the friction coefficient tended to decrease gradually with the increasing rotation speed; when the rotation speed was 550 n/min, the average value of friction coefficient reached 0.5. Among the Al_2O_3 matrix composites the friction coefficient of Al_2O_3/TiC was a little lower than others. When the rotation was 550 n/min, the coefficient was 0.42.

The friction coefficient curves of Al_2O_3/TiC, Al_2O_3/(W,Ti)C and Al_2O_3/Ti(C,N) were shown in Fig. 8 which was tested with increasing load and rotation speed was fixed at 550 rpm. It

Table 2
Mechanical properties of the alumina matrix composite ceramics.

Materials	Phase content (vol.%)				Fracture toughness (MPa $m^{1/2}$)	Fracture strength (MPa)	Hardness (GPa)	Density (g/cm^3)	Residual porosity (%)
	Al_2O_3	TiC	(W,Ti)C	Ti(C,N)					
Al_2O_3/TiC	45	55			7.74 ± 0.58	889 ± 92	19.1 ± 0.1	4.29 ± 0.05	0.5 ± 0.011
Al_2O_3/(W,Ti)C	66		34		5.1 ± 0.32	850 ± 64	21.5 ± 0.13	5.41 ± 0.52	0.8 ± 0.013
Al_2O_3/Ti(C,N)	50			50	4.9 ± 0.29	880 ± 73	21 ± 0.11	3.98 ± 0.47	1.3 ± ± 0.017

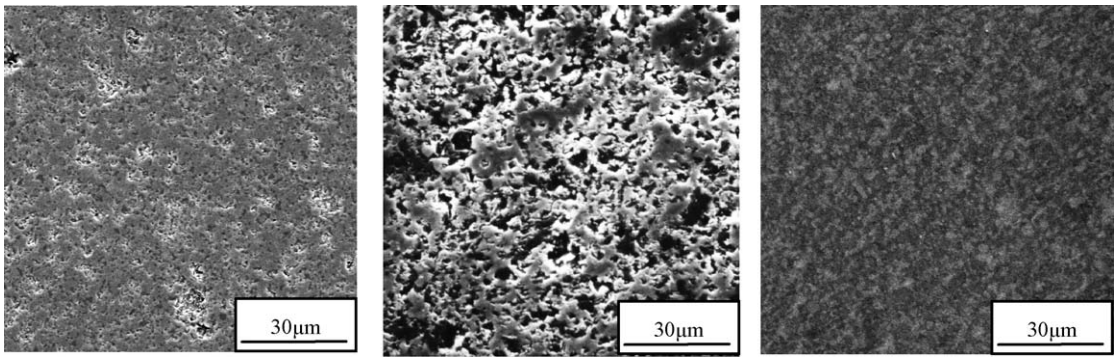

Fig. 5. The SEM micrographs of polishing surfaces of alumina matrix composite.

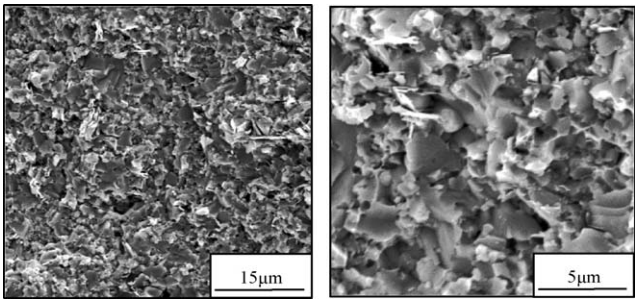

Fig. 6. The SEM micrographs of fracture surfaces of alumina matrix composite.

showed that the friction coefficients presented downtrend from 0.8 to about 0.4 with load increasing from 10 N to 70 N. When the load were 70–150 N, the friction coefficient of Al_2O_3 matrix composites were between 0.4 and 0.5. The friction coefficients of Al_2O_3 matrix composites were just about equal when the rotation speed was 550 n/min and load was 150 N.

The wear resistance of ceramic went direct ratio with $HV^{1/2} \cdot K_{IC}^{3/4}$ (HV is Vickers hardness; K_{IC} is fracture toughness). After surveyed and calculated according to formula (1), the wear rate curves of Al_2O_3/TiC, Al_2O_3/(W,Ti)C and Al_2O_3/Ti(C,N) were shown in Fig. 9 at different rotation speed when the load was 150 N.

It showed that the wear rate trend curves of Al_2O_3 matrix composites were different with increasing rotation. The wear rate of Al_2O_3/TiC tended to decrease gradually with the

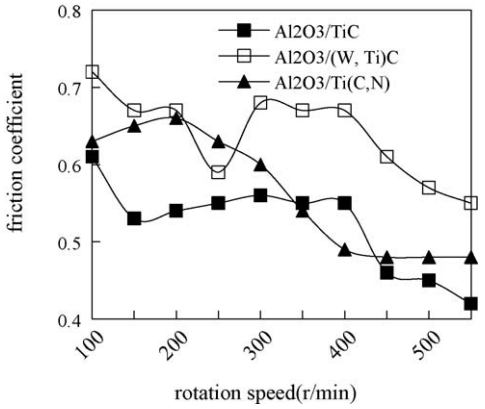

Fig. 7. The friction coefficient of Al_2O_3 matrix ceramic composite with different rotation speed (load = 90 N).

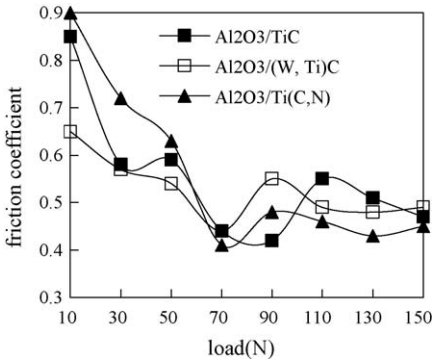

Fig. 8. The friction coefficient of Al_2O_3 matrix ceramic composite with different pressure (rotation speed = 550 rpm).

increasing rotating speed, its value was downward from 8.87×10^{-9} cm^3/(N m) to 3.1×10^{-9} cm^3/(N m). The results showed that the Al_2O_3/TiC composite has low wear rate and good wear resistance, especially under high rotation speed. The wear rate of Al_2O_3/(W,Ti)C tended to decrease quickly from 25.6×10^{-9} cm^3/(N m) to 1.28×10^{-9} cm^3/(N m) when the rotation speed increased from 100 rpm to 400 rpm. When the rotation speed is 400 n/min, it dropped to its minimum value, and then increases a little as the rotation speed increased continuously. It showed that the sliding friction of Al_2O_3/(W,Ti)C was well at a middle and high speed, and its wear resistance was better at high speed than at low speed.

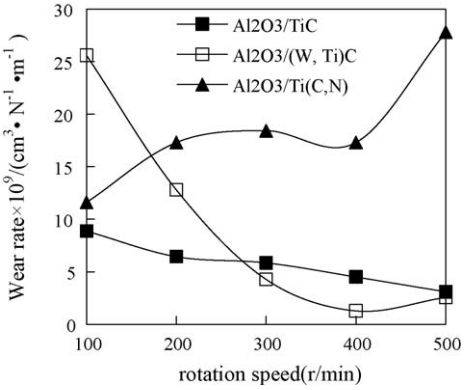

Fig. 9. The wear rate of Al_2O_3 matrix ceramic composite with different rotation speed (load = 150 N).

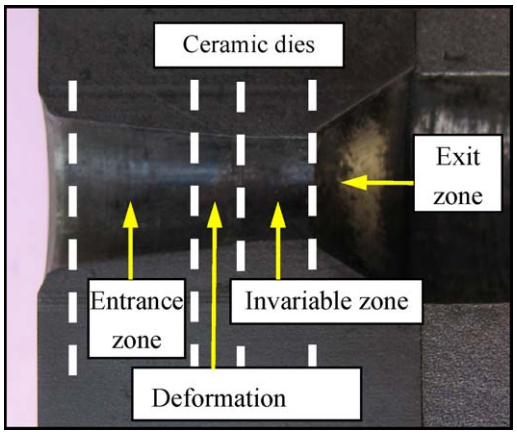

Fig. 10. Worn bore surfaces of ceramic die. (a) Entrance zone; (b) deformation zone; (c) invariable zone; (d) exit zone.

However the experiment record of Al_2O_3/Ti(C,N) was totally different; its wear volume got larger and larger when the rotation speed increased from 100 rpm to 500 rpm, its wear rate was 11.6×10^{-9} cm^3/(N m) and then increased to 27.8×10^{-9} cm^3/(N m) at high speed. It showed that Al_2O_3/Ti(C,N) was unfit for high speed grinding. The wear resistance of Al_2O_3/Ti(C,N) was worse than those value of Al_2O_3/TiC and Al_2O_3/(W,Ti)C.

3.3. The wear behaviors and mechanisms of alumina matrix ceramics die

The worn bore surfaces of ceramic die were as Fig. 10. The worn micrograph of entrance zone was shown in Fig. 11(a). It showed that the surface of entrance zone was smooth. And there were small pits on the surface. There were no a mass of friction and wear traces in the whole entrance zone.

The worn micrograph of bearing zone was shown in Fig. 11(b). It showed that there were lots of furrows and fallen grains on the surface of bearing zone. The surface was worn badly. It was obvious that the traces brought along wire drawing direction by friction and wear. At some area of the surface, there were some pits due to fallen grains and micro-cracks.

The worn micrograph of invariable zone was shown in Fig. 11(c). It showed that the worn behaviors of invariable zone surface were the same as bearing zone, there were lots of

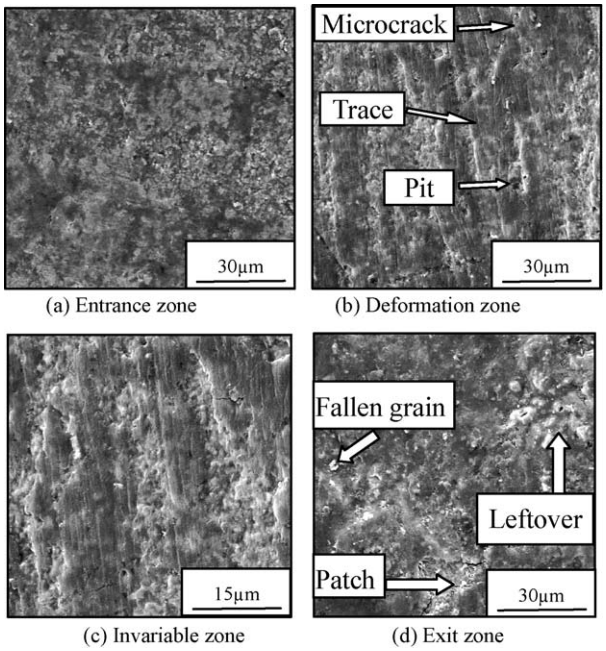

Fig. 11. The micrographs of worn born surfaces in different zone.

furrows and fallen grains. Abrasive wear properties were main worn behaviors. The surface was worn badly and coarse. There was little lubricating leftover on invariable zone. Obviously, the traces brought along wire drawing direction. At some area of the surface, some pits and micro-cracks appeared by fallen grains.

The worn micrograph of exit zone was shown in Fig. 11(d). Figure showed that the worn behaviors of exit zone surface were completely different from others zone, there were some cracks. Main worn behaviors were crushes with fallen grains and no traces appeared on surface. There was some lubricating leftover on surface.

As a whole, the wear and tear behaviors were different in different zones. In entrance zone, the surface did not contact with wire, so the surface was smoothness and only few scratches existed due to wire come into. On the surface of bearing and invariable zone, the wire touched the surface tempestuously, the friction and wear was quite severe, and then lots of physical traces were produced with fallen grains and micro-cracks. In exit zone, the worn behaviors were main

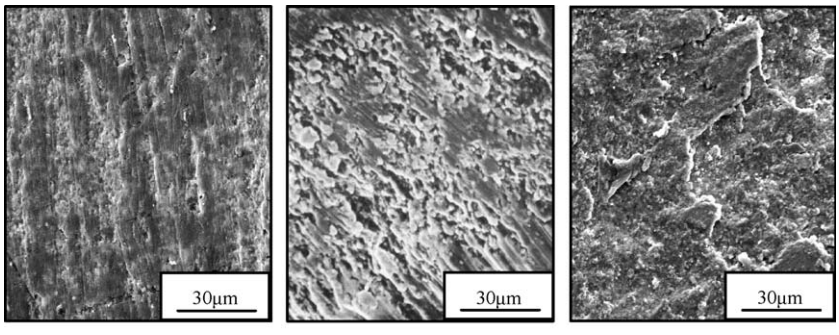

Fig. 12. The micrographs of worn born surfaces in deformation zone with different Al_2O_3 matrix composite.

crushability properties with fallen grains and some lubricating leftover.

Fig. 12 was the SEM micrographics of wear appearance compared with Al_2O_3 matrix composites at deformation zone. Fig. 12(a) was Al_2O_3/TiC, Fig. 12(b) was Al_2O_3/(W,Ti)C and Fig. 12(c) was Al_2O_3/Ti(C,N). Their wear surfaces were all rough and uneven.

Fig. 12(a) showed that the ceramic die happened acute friction with drawn wire. There were lots of furrows and fallen grains on the friction surfaces. From micrograph Fig. 12(b), it showed that a few Al_2O_3 grains peel off from the wear surface of Al_2O_3/(W,Ti)C. The remained (W,Ti)C played an important role on its wear resistance because of its better hardness. From Fig. 12(c), there were distinct scraping traces on the wear surface of Al_2O_3/Ti(C,N). It showed that the wear mechanism of Al_2O_3/Ti(C,N) was mainly brittle peel off in the given experiment.

3.4. The calculation of drawing forces and simulation of drawing process based on FEM

The forces of drawing die were brought by drawn wire. Before simulation, the drawing forces were calculated with mathematical method, the sketch of drawing process is as Fig. 13, and the motor provide the drive in drawing process, and the deformation of wire take place in internal hole. Outside surfaces of die, there is a pre-tightening steel part for preventing the breakage of die. The drawing forces were calculated by formulae (2) and (3):

$$P_a = \sigma_a S_a = \frac{1+\mu/\tan\alpha/2}{\mu/\tan\alpha/2}\left(1-\frac{1}{(q+1)^{\mu/\tan\alpha/2}}\right)\sigma_s S_a \quad (2)$$

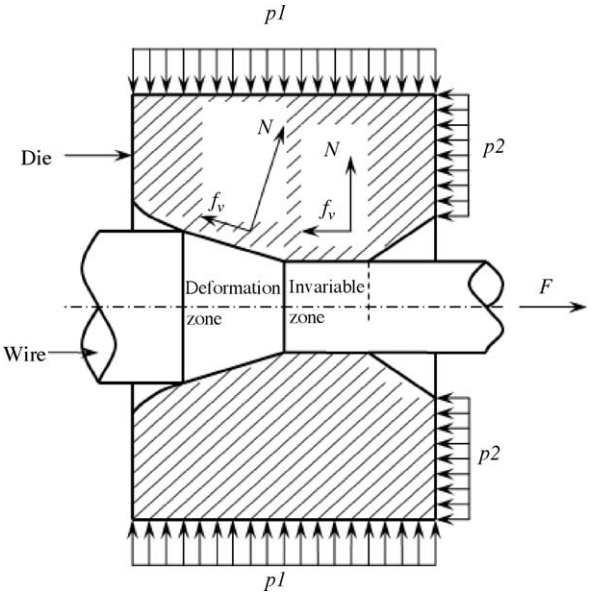

Fig. 13. The forces situation of different zone in drawing process. (a) Boundary conditions; (b) relative movement; (c and d) the friction surfaces of die with wire and steel.

$$P_l = \frac{\pi}{4}\left(1-\frac{1-\sigma_a/\sigma_s}{e^C}\right)\sigma_s D_a^2 \quad (3)$$

The parameter

$$c = \frac{1}{\mu/\tan\alpha/2}\ln\left[\left(1+\frac{\mu}{\tan\alpha/2}\right)\sigma_s - \frac{\mu}{\tan\alpha/2}\sigma_b\right] - 2\ln D_b$$

Note: P_a, the drawing force at the boundary between deformation zone and invariable zone, P_l, the drawing force at the exit zone, σ_a, the drawing stress at the boundary between deformation zone and invariable zone, σ_s, the yield limit of material, μ, the friction coefficient between die and wire, α, the angle at deformation zone, q, the reduction ratio, D_a, the diameter of invariable zone, and S_a, the area of invariable zone.

The drawn wire is 65Mn steel in this example; its diameter was 4.5 mm, which changed to 4 mm after drawing process, with the reduction ratio of $q = 21\%$. The coefficient of friction was $\mu = 0.4$ and the angle at deformation zone was $\alpha = 14^\circ$. According to the formulae (2) and (3) of drawing forces, P_a was 2684 N and P_l was 4219.52 N. Obviously, the drawing force in invariable zone was larger than in deformation zone, and the axial stresses are larger than other stresses. In internal hole, the axial stresses and drawing force becomes large gradually along drawing direction. The maximum value of drawing force happens naturally at the exit of invariable zone.

In order to observe the distribution of inner bore stresses of ceramic die, the geometry models of all structure were established as three quarter of all. So the same properties were evaluated on symmetry surface. The ceramic die and cover steel were tightened together and had no movement. The drawn wire went through inner bore by drawing force. The boundary conditions of drawing process were as Fig. 14(a).

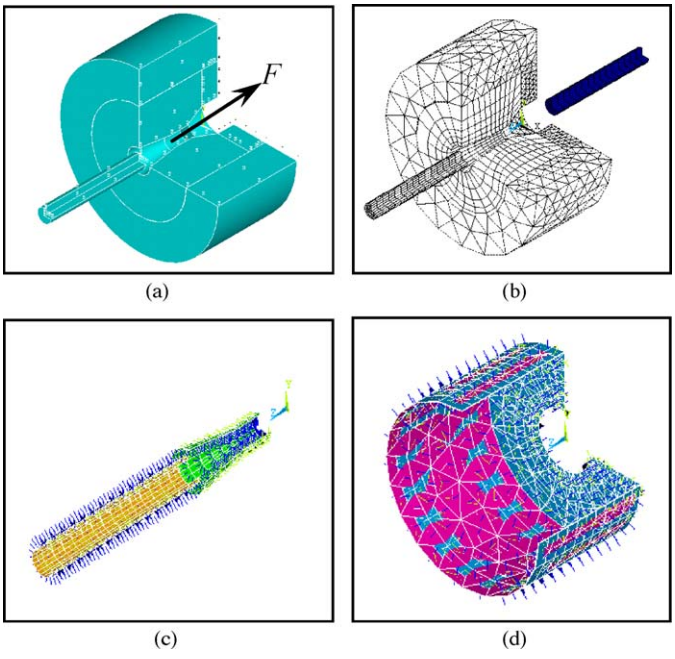

Fig. 14. Properties of drawing process.

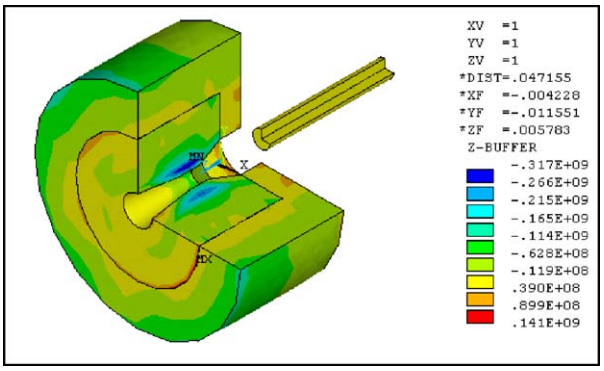

Fig. 15. Axial stresses distribution of ceramic die.

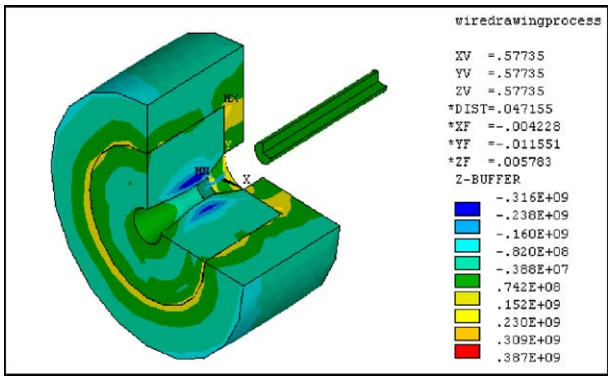

Fig. 17. Primary stresses distribution of ceramic die.

In drawing process, the drawn wire brought on plastic deformation through inner bore because of large drawing force. The relative movement was established as Fig. 14(b).

The static friction happened at outside surface on ceramic die and inside surface of steel. The sliding friction happened at outside surface of drawn wire and inner bore of ceramic die. So the relevant friction surfaces were defined in simulation environment as Fig. 14(c) and (d).

The most common failure of the ceramic drawing die was the wear at the deformation zone and invariable zone owing to the greater drawing stresses. The stress distribution of die was solved by FEM. Fig. 15 was the axial stresses distribution with drawing velocity which was 500 mm/min. It showed that the axial stresses were axisymmetric and the main stresses were press. The great press stresses took place at the deformation zone and invariable zone and the maximum value reached 317 MPa. At the entrance zone and exit zone, the stresses are less than when they were at the deformation zone and invariable zone.

The radial stresses distribution of ceramic dies was as Fig. 16. It was obvious that the radial stresses were larger than axial stresses; the maximum value of press stress was 2030 MPa on the deformation zone surface. The largest press stresses appeared at the deformation zone and invariable zone and the values of stresses descended from deformation zone and invariable zone to entrance zone and exit zone.

The primary stresses distribution of ceramic dies was as Fig. 17. It was obvious that the primary stresses were pressure.

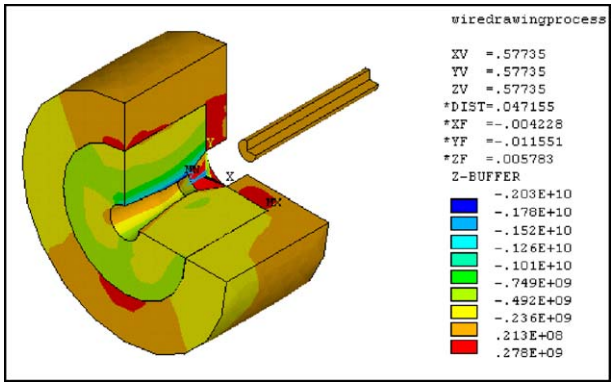

Fig. 16. Radial stresses distribution of ceramic die.

The great press stresses appeared at the deformation zone and invariable zone and the values of stresses descended from deformation zone and invariable zone to entrance zone and exit zone. The maximum value of press stress was 316 MPa on the deformation zone surface.

As a whole, the wear and tear behaviors are different at the different zones. At the entrance zone, the surface did not contact with wire, so the surface is smooth and there are only few scratches due to wire coming into it. On the surface of deformation and invariable zone, the wire touches the surface tempestuously, the friction and wear is quite severe, then lots of mechanism traces are produced with fallen grains and micro cracks. At the exit zone, the worn behaviors are main crushability properties with fallen grains, where there are a lot of lubricating leftovers.

In drawing process, wear mechanisms are different in every zone. The worn surfaces are severe at deformation zone and invariable zone, and the wear mechanism is abrasive primarily with small micro-cracks.

4. Conclusions

The Al_2O_3 matrix ceramic composites with high hardness and good wear resistance have been successfully developed by hot pressing sintering method for the purpose of improving its mechanical properties. The mechanical properties of ceramic dies were tested and the experiment was carried out on wire drawing testing equipment, and the wear mechanisms of the ceramic dies have been studied extensively. It has been found that:

1. The Al_2O_3/TiC, Al_2O_3/(W,Ti)C and Al_2O_3/Ti(C,N) have good hardness and flexure strength. All the tested mechanical properties of Al_2O_3 matrix ceramic dies showed it is suitable for using as drawing dies.
2. The friction coefficient of Al_2O_3 matrix ceramic dies was about 0.4–0.5 when the rotation speed was 550 n/min. The Al_2O_3 matrix ceramics dies had good wear resistance because of low wear rate in experiment. The curves of wear rate of Al_2O_3 matrix composites were different with increasing rotation. The wear rate of Al_2O_3/TiC and Al_2O_3/(W,Ti)C tended to decrease gradually with increasing rotating speed. Al_2O_3/Ti(C,N) was unfit for high speed

grinding. The wear resistance of Al_2O_3/Ti(C,N) was a little worse than those of wear resistance of Al_2O_3/TiC and Al_2O_3/(W,Ti)C at high speed.

3. Wear behaviors on bore surfaces of Al_2O_3 matrix ceramic dies were different. The most common failure of the ceramics dies was the wear at the deformation zone and invariable zone owing to the greater pressure. Abrasive and adhesive wear were found to be the predominant wear mechanisms for Al_2O_3 matrix ceramics drawing dies. At deformation zone and invariable zone, the worn surfaces of Al_2O_3/TiC and Al_2O_3/(W,Ti)C showed that acute friction and furrows happened and then followed by micro-cracks. The main wear mechanism of them was abrasive wear. The main wear mechanism of Al_2O_3/Ti(C,N) was brittle peel off.

Acknowledgements

The authors acknowledge the experiments resources Shandong University and the financial support by the Natural Science Foundation of University of Jinan (B0614). The author Yang Xue-feng would like to thanks the support from other teacher for helping investigate and research.

References

[1] Z.M. Zhang, H.S. Shen, F.H. Sun, X.C. He, Y.Z. Wan, Fabrication and application of chemical vapor deposition diamond-coated drawing dies, Diamond and Related Materials 10 (2001) 33–38.
[2] X.F. Yang, J.X. Deng, Materials and structure of the wire drawing dies, Tool Engineering 38 (8) (2004) 64–69 (in Chinese).
[3] X.F. Yang, J.X. Deng, J. Zhou, S.Q. Yao, C. Li, Friction and wear behaviors of three ceramic composite, Key Engineering Materials 315/316 (2006) 94–97.
[4] X.F. Yang, J.X. Deng, S.Q. Yao, Friction and wear behaviors of Al_2O_3/TiC ceramic composite using as wire drawing dies, Journal of the Chinese Ceramic Society 33 (12) (2005) 1522–1526.
[5] S. Hollinger, E. Depraetere, O. Giroux, Wear mechanism of tungsten carbide dies during wet drawing of steel tyre cords, Wear 255 (2003) 1291–1299.
[6] X.-F. Yang, J.-X. Deng, H. Wang, X.-B. Ze, Wear behaviors and lubrication medium of TiC/Al_2O_3 ceramic wire drawing dies, Transactions of Nonferrous Metals Society of China 17 (1) (2007) s663–s666.
[7] J.X. Deng, X.F. Yang, J.H. Wang, Wear mechanisms of Al_2O_3/TiC/Mo/Ni ceramic wire-drawing dies, Materials Science and Engineering 424 (1–2) (2006) 347–354.

Yang Xue-feng, 1977, PhD, specialized on wear and friction behaviours of ceramics composites, the computer simulation technology, design and manufacture of mechanism.